

Effective Field Theory of ${}^3\text{He}$

Shung-ichi Ando and Michael C. Birse

Theoretical Physics Group, School of Physics and Astronomy,

The University of Manchester, Manchester, M13 9PL, UK

${}^3\text{He}$ and the triton are studied as three-body bound states in the effective field theory without pions. We study ${}^3\text{He}$ using the set of integral equations developed by Kok *et al.* which includes the full off-shell T -matrix for the Coulomb interaction between the protons. To leading order, the theory contains: two-body contact interactions whose renormalized strengths are set by the NN scattering lengths, the Coulomb potential, and a three-body contact interaction. We solve the three coupled integral equations with a sharp momentum cutoff, Λ , and find that a three-body interaction is required in ${}^3\text{He}$ at leading order, as in the triton. It also exhibits the same limit-cycle behavior as a function of Λ , showing that the Efimov effect remains in the presence of the Coulomb interaction. We also obtain the difference between the strengths of the three-body forces in ${}^3\text{He}$ and the triton.

I. INTRODUCTION

Since Weinberg first proposed applying the ideas of effective field theory (EFT) to nuclear forces [1], much effort has gone into this approach. (For reviews, see Refs. [2–4].) Although there is still some debate about how best to implement it at energies where pion-exchange forces are resolved, the picture is clearer at lower energies. Here few-nucleon systems can be described by a “pionless” EFT based on two- and three-body contact interactions [5–8]. The resulting expansion of the two-body force is just that of the effective-range expansion [9], but the EFT framework makes it possible to extend this consistently to other effective operators and three-body forces.

This theory has been applied extensively to two-body systems, where it has been extended to include the effects of the Coulomb interaction on proton-proton scattering [10–14]. In that system, it corresponds to a distorted-wave or “modified” version of the effective-range expansion [9].

Three-body systems have also been studied in the pionless EFT [5, 8]. In these, exchange of one particle between an interacting pair and the third particle leads to a long-range force that can be either attractive or repulsive depending on the overall symmetry of the wave function. Attractive channels, such as the triton, display the Efimov effect [15] in the limit of infinite two-body scattering length. This consists of an infinite tower of bound states with energies in a constant ratio. It results from a discrete scale invariance in these systems and corresponds to a limit cycle of the renormalisation group (RG) for the contact three-body force [16].

The ${}^3\text{He}$ nucleus is of particular interest since it can potentially provide access to properties of the neutron that require a polarised target. It should be possible to describe its low-energy properties within the pionless EFT, extended to include the Coulomb interaction. However the only previous application of the theory to the pd system is in the work of Rupak and Kong, who treated Coulomb effects perturbatively and only considered the spin-3/2 channel [17].

A nonperturbative treatment may not be essential for the ${}^3\text{He}$ ground state, given the typical momenta in the wave function. However it will be necessary if the EFT is to be extended to describe pd scattering near threshold. Also, it is needed to answer the question of whether the Efimov effect survives in the presence of the Coulomb interaction. Arguments based on the degrees of the singularities in the potentials suggest it should and this has been checked by Hammer and Higa for a simpler two-body model [18]. However it has not previously been confirmed in a three-body system.

Like most other EFT studies of the triton and other three-body systems [3], our treatment is formulated in terms of a set of integral equations. However a quite different approach, based on the resonating-group method, was recently applied to three- and four-nucleon systems by Kirscher *et al.* [19]. While this also treats the Coulomb interaction to all orders, limitations on the range of cutoffs mean that it is not able to test whether the Efimov effect occurs.

Here we report the results of a study of ${}^3\text{He}$ in the pionless EFT with the Coulomb interaction treated nonperturbatively. Our approach is based on that used by Kok *et al.* [20] to study ${}^3\text{He}$ with separable potentials and the full off-shell Coulomb T -matrix. The resulting set of integral equations is very similar to that developed by Skornyakov and ter-Martirosian [21] which have more recently been used in EFT studies of the triton and other

three-body systems [3].

Our results show that the Efimov effect does indeed occur in the presence of the Coulomb interaction. We also determine the strength of the three-body force needed to reproduce observed ${}^3\text{He}$ binding energy. The difference between this and the corresponding force needed for the triton is of the expected size for an electromagnetic effect.

II. LAGRANGIAN

In the pionless EFT, the strong forces between nucleons are described by two- and three-body contact interactions. In the present context it is convenient to represent the two-body interactions in terms of dibaryon fields. The resulting effective Lagrangian for the three-nucleon system can be written as [8, 22]

$$\mathcal{L} = \mathcal{L}_N + \mathcal{L}_s + \mathcal{L}_t + \mathcal{L}_3, \quad (1)$$

where \mathcal{L}_N is the standard one-nucleon Lagrangian in the heavy-baryon formalism,

$$\mathcal{L}_N = N^\dagger \left\{ iv \cdot D + \frac{1}{2m_N} [(v \cdot D)^2 - D^2] \right\} N. \quad (2)$$

Here v^μ is a velocity vector satisfying a condition $v^2 = 1$, D_μ is the covariant derivative, and m_N is the nucleon mass. The terms \mathcal{L}_s and \mathcal{L}_t are dibaryon effective Lagrangian for spin singlet and triplet parts, respectively, and these read

$$\mathcal{L}_s = s_a^\dagger \{ iv \cdot D + \Delta_{s(a)} \} s_a - y_s \left\{ s_a^\dagger \left[N^T P_a^{(1S_0)} N \right] + h.c. \right\}, \quad (3)$$

$$\mathcal{L}_t = t_i^\dagger \{ iv \cdot D + \Delta_t \} t_i - y_t \left\{ t_i^\dagger \left[N^T P_i^{(3S_1)} N \right] + h.c. \right\}, \quad (4)$$

where s_a and t_i are the corresponding dibaryon fields. The strengths of the corresponding two-body interactions depend on $\Delta_{s(a)}$ and Δ_t , the mass differences between the dibaryons and two nucleons, and y_s and y_t , the coupling constants for the dibaryon-nucleon-nucleon vertices. The projection operators for the two-nucleon 1S_0 and 3S_1 states are

$$P_a^{(1S_0)} = \frac{1}{\sqrt{8}} \tau_2 \tau_a \sigma_2, \quad P_i^{(3S_1)} = \frac{1}{\sqrt{8}} \tau_2 \sigma_2 \sigma_i, \quad (5)$$

where τ_a and σ_i are Pauli matrices for isospin and spin, respectively.

The present work is based on the leading-order (LO) terms in the expansion of this EFT of Q . Here Q stands for any of the low-energy scales in the problem: the relative

momenta, $1/a$ where a is any of the NN scattering lengths, and the inverse of the Bohr radius $\kappa = \alpha_{\text{EM}} m_N/2$. More precisely, we keep all terms of order Q^{-1} , noting that the strong attraction in the NN S waves enhances the wave functions near the origin and hence promotes contact interactions proportional to $1/a$ or κ to this order [6, 7, 23, 24].

The Coulomb interaction leads to a well-known logarithmic divergence in the NN loop integrals [10–12]. This is renormalised by a LO counterterm that contributes to the pp scattering length. Given that we need to include isospin breaking in this channel, we have also taken account of charge-independence breaking between the 1S_0 np and nn scattering lengths, even though this is formally of higher order. This allows us to present the general structures of the three-body equations, which will be needed for extensions of this work to higher orders. We have not included the neutron-proton mass difference which is not only of higher order but is smaller than might be expected as a result of cancellations between electromagnetic and strong contributions [25]. To the order we work, observables depend only on the combinations $\Delta_{s(a)}/y_s^2$ and so we have chosen to leave the couplings y_s isospin-invariant.

The three-body force is expressed as a dibaryon-nucleon contact interaction. It is given by the effective Lagrangian,

$$\begin{aligned} \mathcal{L}_3 = \frac{m_N H(\Lambda)}{3\Lambda^2} \Big\{ & y_t^2 N^\dagger(\vec{\sigma} \cdot \vec{t})^\dagger (\vec{\sigma} \cdot \vec{t}) N - y_s y_t [N^\dagger(\vec{\sigma} \cdot \vec{t})^\dagger (\vec{\tau} \cdot \vec{s}) N + h.c.] \\ & + y_s^2 N^\dagger(\vec{\tau} \cdot \vec{s})^\dagger (\vec{\tau} \cdot \vec{s}) N \Big\}, \end{aligned} \quad (6)$$

where $H(\Lambda)$ is the coupling constant, which runs with the scale Λ of the cutoff we impose on the coupled integral equations. Note that this interaction contributes only to three-body channels with total spin 1/2 and total isospin 1/2.

The building blocks needed to construct the three-body integral equations from the Lagrangian are as follows. In the one-body sector, we have the non-relativistic nucleon propagator,

$$iS_N(p) = \frac{i}{p_0 - \frac{\vec{p}^2}{2m_N} + i\epsilon}. \quad (7)$$

In the two-body sector, we need the dressed dibaryon propagators with and without the Coulomb interaction. The propagators for the np and nn channels, which have no Coulomb

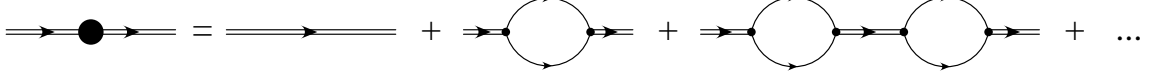


FIG. 1: Diagrams for the dressed dibaryon propagator, denoted by the double line with filled circle. Single lines represent nucleon propagators; double lines undressed dibaryon propagators.

interaction, are represented by the diagrams in Fig. 1 and are given by

$$iD_{s,t} \left(E - \frac{3q^2}{4m_N} \right) = \frac{4\pi}{m_N y_{s,t}^2} \frac{-i}{-\mu - \frac{4\pi\Delta_{s,t}}{m_N y_{s,t}^2} + \sqrt{\frac{3}{4}q^2 - m_N E - i\epsilon + i\epsilon}}. \quad (8)$$

The two-nucleon loop diagrams here have been dimensionally regularised using the PDS scheme with the subtraction scale μ . The dependence on this can be removed by renormalising the constants $4\pi\Delta_{s,t}/(m_N y_{s,t}^2)$ using

$$\mu + \frac{4\pi\Delta_{s(np)}}{m_N y_s^2} = \frac{1}{a_{np}}, \quad \mu + \frac{4\pi\Delta_{s(nn)}}{m_N y_s^2} = \frac{1}{a_{nn}}, \quad \mu + \frac{4\pi\Delta_t}{m_N y_t^2} = \gamma, \quad (9)$$

where a_{np} and a_{nn} are the scattering lengths for the spin-singlet np and nn channels, respectively, and γ is related to the deuteron binding energy B_2 through $\gamma = \sqrt{m_N B_2}$. Working to leading order, we neglect corrections from the effective ranges.

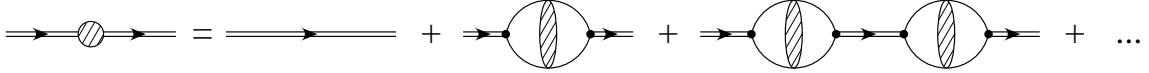


FIG. 2: Diagrams for dressed dibaryon propagator for the pp channel, denoted by the double line with shaded circle. The shaded ovals here represent the two-nucleon Green's function dressed with the Coulomb interaction.

In the pp channel, the Coulomb interaction dresses the two-nucleon Green's function in the bubble diagram for the dressed dibaryon propagator, as shown in Fig. 2. The resulting propagator is given by

$$iD_{s(pp)} \left(E - \frac{3q^2}{4m_N} \right) = \frac{4\pi}{m_N y_s^2} \frac{-i}{-\frac{4\pi\Delta_{s(pp)}^R}{m y_s^2} - 2\kappa H(\kappa/p')}, \quad (10)$$

where

$$H(\eta) = \psi(i\eta) + \frac{1}{2i\eta} - \ln(i\eta), \quad (11)$$

ψ is the logarithmic derivative of the Γ function, and $-ip' = \sqrt{\frac{3}{4}q^2 - m_N E - i\epsilon}$. The renormalised constant $\Delta_{s(pp)}^R$ for the pp channel cancels both the linear and logarithmic divergences of the loop diagram. It is related to the Coulomb scattering length a_C by

$$\frac{1}{a_C} = \frac{4\pi\Delta_{s(pp)}^R}{m_N y_s^2} = \frac{4\pi\Delta_{s(pp)}}{m_N y_s^2} + \mu - 2\kappa \left[1 - C_E + \ln\left(\frac{\mu}{4\kappa}\right) \right], \quad (12)$$

where $C_E = 0.577215 \dots$ is Euler's constant. Note that the logarithmic divergence means that it is impossible to make a model-independent decomposition of $1/a_C$ into strong and electromagnetic contributions [10–12]. This implies that within this EFT there is no unambiguous way to separate Coulomb from other isospin-breaking effects.

The final building block for the integral equations is the off-shell Coulomb T-matrix. A convenient form for it is the integral representation [26] for negative energies, $k^2/m_N < 0$:

$$\langle \mathbf{p}' | T_C(k^2/m_N) | \mathbf{p} \rangle = \frac{e^2}{(\mathbf{p}' - \mathbf{p})^2} \left[1 - 4i\eta \int_0^1 dt \frac{t^{i\eta}}{4t - (1-t)^2(x^2 - 1)} \right], \quad (13)$$

where $\eta = \kappa/k$ and

$$x^2 = 1 + \frac{(p'^2 - k^2)(p^2 - k^2)}{k^2(\mathbf{p}' - \mathbf{p})^2}. \quad (14)$$

III. INTEGRAL EQUATIONS

Now we construct the integral equations for scattering of a third nucleon off a deuteron, concentrating on the channels where the third nucleon is in an S wave, and the total spin and isospin of the three particles are both $1/2$. The negative-energy solutions of these describe the bound triton and ${}^3\text{He}$ states.

We work the center of mass frame for the Nd scattering and use the notation of Bedaque *et al.* [8]. In the isospin-symmetric case, this process can be described by an amplitude $a(p, k)$ for scattering into states with a 3S_1 dibaryon, and $b(p, k)$ for scattering into those with a 1S_0 dibaryon. Here k denotes the initial (on-shell) relative momentum of the deuteron and the third nucleon, and p the final (off-shell) momentum.

The amplitudes satisfy coupled integral equations which can be represented diagrammatically as in Fig. 3. The kernels of these equations consist of two terms: one-nucleon-exchange, which provides a long-range force between the dibaryon and the third nucleon, and the three-body contact interaction.

In the limit of infinite two-body scattering lengths (and zero deuteron binding energy) the long-range force is scale-independent. It is this feature that leads to the Efimov effect in channels where the force is attractive.

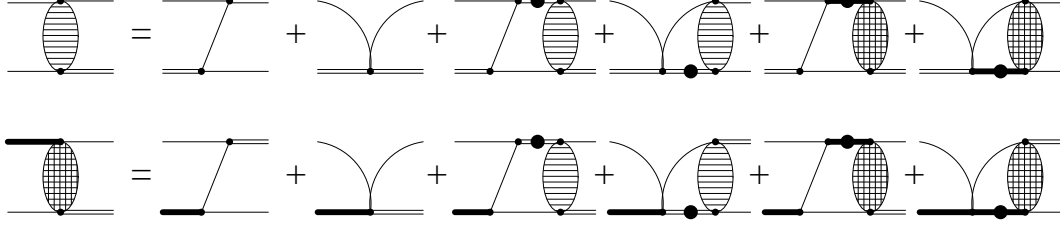


FIG. 3: Diagrams corresponding to the coupled integral equations for nucleon-dibaryon scattering. Thin lines denote nucleons, double and thick lines 3S_1 and 1S_0 dibaryons. Those with filled circles are dressed dibaryon propagators, as in Fig. 1. Ovals with stripes denote the off-shell amplitude $a(p, k)$ with initial and final spin-triplet dibaryons, and those with cross stripes the amplitude $b(p, k)$ with initial spin-triplet and final spin-singlet dibaryon fields.

When we include the Coulomb interaction, isospin symmetry is broken and we must introduce separate amplitudes $b_+(p, k)$ and $b_0(p, k)$ for pd scattering into states with 1S_0 pp and np dibaryons, respectively. These and $a(p, k)$ satisfy a set of three coupled integral equations. For completeness, we also present the corresponding set of three equations that arise when we allow for isospin-breaking effects in the nd case, involving the amplitude $b_-(p, k)$ for states with nn dibaryons. As already mentioned, these are not essential for the present LO calculations but will be needed for extensions to higher orders.

A. Integral equations for the nd channel

Before presenting the equations for pd scattering, we first look at the simpler equations for nd scattering. Allowing for isospin breaking in the scattering lengths, the three integral

equations for the $S = 1/2$, $T = 1/2$ channel are

$$\begin{aligned}
a(p, k) = & K^{(a)}(p, k; E) + 2 \frac{H(\Lambda)}{\Lambda^2} \\
& + \frac{1}{\pi} \int_0^\Lambda dq q^2 \left[K^{(a)}(p, q; E) + 2 \frac{H(\Lambda)}{\Lambda^2} \right] \frac{a(q, k)}{-\gamma + \sqrt{\frac{3}{4}q^2 - mE}} \\
& + \frac{1}{\pi} \int_0^\Lambda dq q^2 \left[K^{(a)}(p, q; E) + \frac{2}{3} \frac{H(\Lambda)}{\Lambda^2} \right] \frac{b_0(q, k)}{-\frac{1}{a_{np}} + \sqrt{\frac{3}{4}q^2 - mE}} \\
& + \frac{2}{\pi} \int_0^\Lambda dq q^2 \left[K^{(a)}(p, q; E) + \frac{2}{3} \frac{H(\Lambda)}{\Lambda^2} \right] \frac{b_-(q, k)}{-\frac{1}{a_{nn}} + \sqrt{\frac{3}{4}q^2 - mE}}, \quad (15)
\end{aligned}$$

$$\begin{aligned}
b_0(p, k) = & 3K^{(a)}(p, k; E) + 2 \frac{H(\Lambda)}{\Lambda^2} \\
& + \frac{1}{\pi} \int_0^\Lambda dq q^2 \left[3K^{(a)}(p, q; E) + 2 \frac{H(\Lambda)}{\Lambda^2} \right] \frac{a(q, k)}{-\gamma + \sqrt{\frac{3}{4}q^2 - mE}} \\
& + \frac{1}{\pi} \int_0^\Lambda dq q^2 \left[-K^{(a)}(p, q; E) + \frac{2}{3} \frac{H(\Lambda)}{\Lambda^2} \right] \frac{b_0(q, k)}{-\frac{1}{a_{np}} + \sqrt{\frac{3}{4}q^2 - mE}} \\
& + \frac{2}{\pi} \int_0^\Lambda dq q^2 \left[K^{(a)}(p, q; E) + \frac{2}{3} \frac{H(\Lambda)}{\Lambda^2} \right] \frac{b_-(q, k)}{-\frac{1}{a_{nn}} + \sqrt{\frac{3}{4}q^2 - mE}}, \quad (16)
\end{aligned}$$

$$\begin{aligned}
b_-(p, k) = & 3K^{(a)}(p, k; E) + 2 \frac{H(\Lambda)}{\Lambda^2} \\
& + \frac{1}{\pi} \int_0^\Lambda dq q^2 \left[3K^{(a)}(p, q; E) + 2 \frac{H(\Lambda)}{\Lambda^2} \right] \frac{a(q, k)}{-\gamma + \sqrt{\frac{3}{4}q^2 - mE}} \\
& + \frac{1}{\pi} \int_0^\Lambda dq q^2 \left[K^{(a)}(p, q; E) + \frac{2}{3} \frac{H(\Lambda)}{\Lambda^2} \right] \frac{b_0(q, k)}{-\frac{1}{a_{np}} + \sqrt{\frac{3}{4}q^2 - mE}} \\
& + \frac{2}{\pi} \int_0^\Lambda dq q^2 \left[\frac{2}{3} \frac{H(\Lambda)}{\Lambda^2} \right] \frac{b_-(q, k)}{-\frac{1}{a_{nn}} + \sqrt{\frac{3}{4}q^2 - mE}}, \quad (17)
\end{aligned}$$

where

$$K^{(a)}(p, q; E) = \frac{1}{2pq} \ln \left(\frac{p^2 + q^2 + 2pq - m_N E}{p^2 + q^2 - 2pq - m_N E} \right). \quad (18)$$

If we set $a_{nn} = a_{np}$ and $b_0 = b_- = b$, these reduce to the isospin-symmetric forms of the equations in Ref. [8].

The integrals over the relative momentum q are all cut off at $q = \Lambda$. The resulting dependence on Λ can be cancelled by the three-body force, whose strength is $H(\Lambda)/\Lambda^2$.

B. Integral equations for the pd channel

We now turn to the corresponding equations for pd scattering. These differ from the ones in the previous subsection by having b_+ instead of b_- and, more importantly, adding the Coulomb interaction between the two protons. They can be obtained from the equations developed by the Groningen group [20], by omitting the separable form factors and instead imposing a sharp cutoff on the relative momenta.

The Coulomb interaction leads to additional long-range terms in the kernels of these equations. The diagrams for the full long-range kernel are shown in Fig. 4. The one-nucleon exchange term of diagram (a) is supplemented by diagram (b) if a proton is exchanged, and by (c) for neutron exchange. Finally, diagram (d) represents the Coulomb interaction between an np dibaryon and a proton.

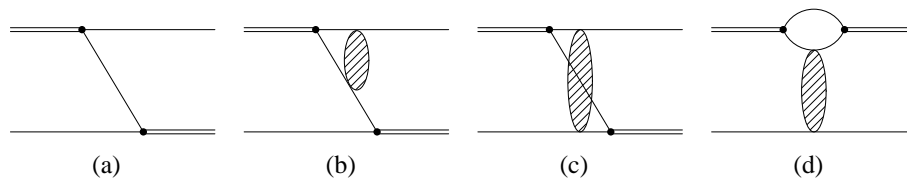


FIG. 4: Diagrams corresponding to the long-range terms in the kernel for pd scattering. Here, the shaded oval denotes the off-shell Coulomb T -matrix (since contributions where the two protons do not interact are already contained in (a)). Diagram (b) has been shown for the case of an initial np dibaryon and a final pp one. The corresponding diagram for the inverse process is the mirror image of this.

The coupled integral equations can be written

$$\begin{aligned}
a(p, k) = & K^{(a)}(p, k; E) + K^{(c)}(p, k; E) + 2K^{(d)}(p, k; E) + 2 \frac{H(\Lambda)}{\Lambda^2} \\
& + \frac{1}{\pi} \int_0^\Lambda dq q^2 \left[K^{(a)}(p, q; E) + K^{(c)}(p, k; E) + 2K^{(d)}(p, k; E) + 2 \frac{H(\Lambda)}{\Lambda^2} \right] \\
& \quad \times \frac{a(q, k)}{-\gamma + \sqrt{\frac{3}{4}q^2 - mE}} \\
& + \frac{1}{\pi} \int_0^\Lambda dq q^2 \left[K^{(a)}(p, q; E) + K^{(c)}(p, k; E) + \frac{2}{3} \frac{H(\Lambda)}{\Lambda^2} \right] \frac{b_0(q, k)}{-\frac{1}{a_{np}} + \sqrt{\frac{3}{4}q^2 - mE}} \\
& + \frac{2}{\pi} \int_0^\Lambda dq q^2 \left[K^{(a)}(p, k; E) + K_{13}^{(b)}(p, k; E) + \frac{2}{3} \frac{H(\Lambda)}{\Lambda^2} \right] \frac{b_+(q, k)}{-\frac{1}{a_C} - 2\kappa H(\kappa/p')},
\end{aligned} \tag{19}$$

$$\begin{aligned}
b_0(p, k) = & 3K^{(a)}(p, k; E) + 3K^{(c)}(p, k; E) + 2 \frac{H(\Lambda)}{\Lambda^2} \\
& + \frac{1}{\pi} \int_0^\Lambda dq q^2 \left[3K^{(a)}(p, q; E) + 3K^{(c)}(p, q; E) + 2 \frac{H(\Lambda)}{\Lambda^2} \right] \frac{a(q, k)}{-\gamma + \sqrt{\frac{3}{4}q^2 - mE}} \\
& - \frac{1}{\pi} \int_0^\Lambda dq q^2 \left[K^{(a)}(p, q; E) + K^{(c)}(p, q; E) + 2K^{(d)}(p, q; E) - \frac{2}{3} \frac{H(\Lambda)}{\Lambda^2} \right] \\
& \quad \times \frac{b_0(q, k)}{-\frac{1}{a_{np}} + \sqrt{\frac{3}{4}q^2 - mE}} \\
& + \frac{2}{\pi} \int_0^\Lambda dq q^2 \left[K^{(a)}(p, q; E) + K_{13}^{(b)}(p, q; E) + \frac{2}{3} \frac{H(\Lambda)}{\Lambda^2} \right] \frac{b_+(q, k)}{-\frac{1}{a_C} - 2\kappa H(\kappa/p')},
\end{aligned} \tag{20}$$

$$\begin{aligned}
b_+(p, k) = & 3K^{(a)}(p, k; E) + 3K_{31}^{(b)}(p, k; E) + 2 \frac{H(\Lambda)}{\Lambda^2} \\
& + \frac{1}{\pi} \int_0^\Lambda dq q^2 \left[3K^{(a)}(p, q; E) + 3K_{31}^{(b)}(p, q; E) + 2 \frac{H(\Lambda)}{\Lambda^2} \right] \frac{a(q, k)}{-\gamma + \sqrt{\frac{3}{4}q^2 - mE}} \\
& + \frac{1}{\pi} \int_0^\Lambda dq q^2 \left[K^{(a)}(p, k; E) + K_{31}^{(b)}(p, q; E) + \frac{2}{3} \frac{H(\Lambda)}{\Lambda^2} \right] \frac{b_0(q, k)}{-\frac{1}{a_{np}} + \sqrt{\frac{3}{4}q^2 - mE}} \\
& + \frac{2}{\pi} \int_0^\Lambda dq q^2 \left[\frac{2}{3} \frac{H(\Lambda)}{\Lambda^2} \right] \frac{b_+(q, k)}{-\frac{1}{a_C} - 2\kappa H(\kappa/p')},
\end{aligned} \tag{21}$$

where $K^{(a)}$ is the one-nucleon exchange kernel defined in Eq. (18) above, and $K_{31}^{(b)}$, $K_{13}^{(b)}$, $K^{(c)}$, and $K^{(d)}$ are the pieces corresponding to the Coulomb diagrams (b), (c), (d) in Fig. 4. (In $K_{31}^{(b)}$ and $K_{13}^{(b)}$, the subscripts 1 and 3 refer to initial and final dibaryons, 1 denoting np and 3 pp .)

In diagram (b), the dibaryon-nucleon-nucleon vertex projects out only the S -wave part of the Coulomb T-matrix. This considerably simplifies the corresponding terms in the equations by reducing the number variables that need to be integrated from six to two. The corresponding terms in the kernels are

$$K_{13}^{(b)}(p, q; E) = \frac{1}{2} \int_{-1}^1 dy \frac{\phi_{13}^{(b)}(p, q, y; E)}{p^2 + q^2 - mE + pqy}, \quad (22)$$

$$K_{31}^{(b)}(p, q; E) = \frac{1}{2} \int_{-1}^1 dy \frac{\phi_{31}^{(b)}(p, q, y; E)}{p^2 + q^2 - mE + pqy}, \quad (23)$$

where $y = \hat{p} \cdot \hat{q} = \cos \theta$ and

$$\phi_{13}^{(b)}(p, q, y; E) = -\frac{4\kappa\beta'}{p'^2 + \beta'^2} \int_0^1 dt t^{\kappa/\beta'} \frac{1}{1 + t^2 - 2 \left(\frac{p'^2 - \beta'^2}{p'^2 + \beta'^2} \right) t}, \quad (24)$$

$$\phi_{31}^{(b)}(p, q, y; E) = -\frac{4\kappa\beta''}{p''^2 + \beta''^2} \int_0^1 dt t^{\kappa/\beta''} \frac{1}{1 + t^2 - 2 \left(\frac{p''^2 - \beta''^2}{p''^2 + \beta''^2} \right) t}. \quad (25)$$

Here we have defined the momentum variables

$$p' = \left| \mathbf{p} + \frac{1}{2}\mathbf{q} \right|, \quad p'' = \left| \mathbf{q} + \frac{1}{2}\mathbf{p} \right|, \quad \beta' = \sqrt{\frac{3}{4}q^2 - mE}, \quad \beta'' = \sqrt{\frac{3}{4}p^2 - mE}. \quad (26)$$

The kernels for diagrams (c) and (d) involve six dimensional integrals but we can analytically evaluate two of these (over the azimuthal angles). In the case of $K^{(c)}$, it is convenient to introduce the vectors,

$$\mathbf{a} = \mathbf{p} + \mathbf{q}, \quad \mathbf{b} = \mathbf{p} - \mathbf{q}, \quad (27)$$

Choosing axes where \mathbf{a} lies along the z -direction, these can be written

$$\mathbf{a} = a(0, 0, 1), \quad \mathbf{b} = b(\sin \theta'', 0, \cos \theta''), \quad \mathbf{l} = l(\sin \theta' \cos \phi', \sin \theta' \sin \phi', \cos \theta'), \quad (28)$$

in terms of their magnitudes

$$a = \sqrt{p^2 + q^2 + 2pq \cos \theta}, \quad b = \sqrt{p^2 + q^2 - 2pq \cos \theta}, \quad (29)$$

and the angles defined by

$$\sin \theta'' = \frac{2pq \sin \theta}{\sqrt{(p^2 - q^2)^2 + 4p^2 q^2 \sin^2 \theta}}, \quad \cos \theta'' = \frac{p^2 - q^2}{\sqrt{(p^2 - q^2)^2 + 4p^2 q^2 \sin^2 \theta}}. \quad (30)$$

The kernel then becomes

$$\begin{aligned}
K^{(c)}(p, q; E) = & -\frac{\kappa}{\pi} \int_0^\infty dl \int_{-1}^1 d(\cos \theta) \int_{-1}^1 d(\cos \theta') \int_0^1 dt \frac{(\kappa/\beta) t^{\kappa/\beta-1}}{bl \sqrt{d^2 + 4t(1-t)^{-2}l^2\beta^2}} \\
& \times \left(\frac{1}{\cos \theta'' \cos \theta' + \frac{2}{bl} \sqrt{d^2 + 4t(1-t)^{-2}l^2\beta^2}} \frac{1}{\sqrt{1-y_1^2}} \right. \\
& \left. - \frac{1}{\cos \theta'' \cos \theta' - \frac{2}{bl} \sqrt{d^2 + 4t(1-t)^{-2}l^2\beta^2}} \frac{1}{\sqrt{1-y_2^2}} \right), \quad (31)
\end{aligned}$$

where

$$\begin{aligned}
y_{1,2} &= \frac{\sin \theta'' \sin \theta'}{\cos \theta'' \cos \theta' \pm \frac{2}{bl} \sqrt{d^2 + 4t(1-t)^{-2}l^2\beta^2}}, \\
d &= l^2 + p^2 + q^2 + pq \cos \theta - \frac{3}{2}al \cos \theta' - m_N E, \\
\beta^2 &= \frac{3}{4}(l^2 + a^2 + 2al \cos \theta') - m_N E. \quad (32)
\end{aligned}$$

The last term in the kernel, arising from diagram (d), requires the most care in its numerical evaluation. This is because the long-range photon exchange gives rise to a logarithmic IR singularity. In the present work, where we are interested only in bound states, the finite extent of the wave functions helps to regulate this singularity. Calculations of pd scattering amplitudes will, however, require different numerical methods. Following Ref. [20], we split $K^{(d)}$ up into three pieces,

$$K^{(d)}(p, q; E) = K^{(d,V')}(p, q; E) + K^{(d,V'')}(p, q; E) + K^{(d,T-V)}(p, q; E), \quad (33)$$

where $K^{(d,V')}$ and $K^{(d,V'')}$ denote the contributions from singular and nonsingular parts of one-photon exchange, and $K^{(d,T-V)}$ the remaining (also nonsingular) terms from iterating

the Coulomb potential. These have pieces have the forms

$$K^{(d,V')}(p, q; E) = -\frac{\kappa}{4pq\beta'} \ln \left(\frac{p^2 + q^2 + 2pq}{p^2 + q^2 - 2pq} \right), \quad (34)$$

$$\begin{aligned} K^{(d,V'')}(p, q; E) = & -\kappa \int_{-1}^1 d(\cos \theta) \frac{1}{p^2 + q^2 - 2pq \cos \theta} \left\{ \frac{1}{\sqrt{p^2 + q^2 - 2pq \cos \theta}} \right. \\ & \times \left[\arctan \left(\frac{-p^2 + 2q^2 - pq \cot \theta}{2\beta' \sqrt{p^2 + q^2 - 2pq \cos \theta}} \right) \right. \\ & \left. \left. + \arctan \left(\frac{2p^2 - q^2 - pq \cos \theta}{2\beta \sqrt{p^2 + q^2 - 2pq \cos \theta}} \right) \right] - \frac{1}{2\beta'} \right\}, \end{aligned} \quad (35)$$

$$\begin{aligned} K^{(d,T-V)}(p, q; E) = & -\kappa \int_{-1}^1 d(\cos \theta) \frac{1}{p^2 + q^2 - 2pq \cos \theta} \\ & \times \left\{ \frac{1}{\pi} \int_0^\infty dl l^2 \int_{-1}^1 d(\cos \theta') \int_0^1 dt \frac{(\kappa/\beta_l) t^{\kappa/\beta_l - 1}}{D \sqrt{1 - c^2}} \right. \\ & - \frac{1}{\sqrt{p^2 + q^2 - 2pq \cos \theta}} \left[\arctan \left(\frac{-p^2 + 2q^2 pq \cos \theta}{2\beta' \sqrt{p^2 + q^2 - 2pq \cos \theta}} \right) \right. \\ & \left. \left. + \arctan \left(\frac{2p^2 - q^2 - pq \cos \theta}{2\beta \sqrt{p^2 + q^2 - 2pq \cos \theta}} \right) \right] \right\}, \end{aligned} \quad (36)$$

where

$$\begin{aligned} \beta' &= \sqrt{\frac{3}{4}p^2 - m_N E}, \quad \beta = \sqrt{\frac{3}{4}q^2 - m_N E}, \quad \beta_l = \sqrt{\frac{3}{4}l^2 - m_N E}, \\ D &= (l^2 + q^2 + ql \cos \theta - m_N E)(l^2 + p^2 + pl \cos \theta - m_N E) \\ &\quad + 4t(1-t)^{-2} \beta_l^2 (p^2 + q^2 - 2pq \cos \theta), \\ c &= (l^2 + q^2 + ql \cos \theta - m_N E)pl \sin \theta \sin \theta' / D. \end{aligned} \quad (37)$$

IV. NUMERICAL RESULTS FOR BOUND STATES

We solve for the three-body bound states by taking the homogeneous parts of the coupled integral equations and treating them as nonlinear eigenvalue problems,

$$K(E)u = u, \quad (38)$$

where $u^T = (a, b_0, b_\pm)$ and the 3×3 matrices of integral operators $K(E)$ can be extracted from the expressions in the previous section.

To convert $K(E)$ into a matrix we use Gauss-Legendre quadrature to replace the momenta p and q by discrete variables. We have examined three versions of this discretisation, in terms

of variables x defined by: (1) $p = m \tan(x)$ where $m = 140$ MeV, (2) $p = x$ (no change of variable), and (3) $p = m_0 \exp(x)$ where $m_0 = 1$ MeV. The variables p and q run from zero to the cutoff Λ , except in the third of these where we also need to impose a cutoff at the very small momentum m_0 .

We then construct the determinant of the matrix $K(E) - 1$ and search on E to find the energy eigenvalues at which $\det[K(E) - 1] = 0$. For one of these values of E , we then solve the eigenvalue problem Eq. (38) and determine the eigenvector corresponding to the unit eigenvalue of the matrix $K(E)$.

For given values of the two-body input parameters we first set the three-body force $H(\Lambda)$ to zero and adjust the value of the cutoff until the shallowest bound-state eigenvalue reproduces the observed three-body binding energy. Starting from this cutoff, Λ_0 , we then determine the values of $H(\Lambda)$ needed to reproduce this binding energy for other cutoffs.

A. Triton

In this case, we work with the determinant constructed from the homogeneous part of the coupled integral equations in Eqs. (15), (16), and (17). The two-body input is provided by

$$\gamma = 45.703 \text{ MeV}, \quad a_{np} = -23.749 \pm 0.008 \text{ fm [27]}, \quad a_{nn} = -18.5 \pm 0.4 \text{ fm [28]}. \quad (39)$$

We adjust the three-body force to fit the triton binding energy,

$$B_3(^3\text{H}) = 8.48182 \text{ MeV}, \quad (40)$$

which corresponds to a momentum scale $\alpha = \sqrt{m_N B_3} = 89.239$ MeV.

For 16 Gaussian integration points (corresponding to a 48×48 matrix) we find that our results have converged and, for the three choices of variable discussed above, they agree to 6 significant figures.

For $H(\Lambda) = 0$, we reproduce the experimental binding energy with the cutoff $\Lambda_0 = 380.689$ MeV. The values of the three-body force needed for other cutoffs are shown in Fig. 5.

As we take $\Lambda \rightarrow \infty$, the cutoff becomes much larger than the physical scales in the system ($1/a$) and $H(\Lambda)$ displays the limit-cycle behaviour found in Ref. [8]. This reflects

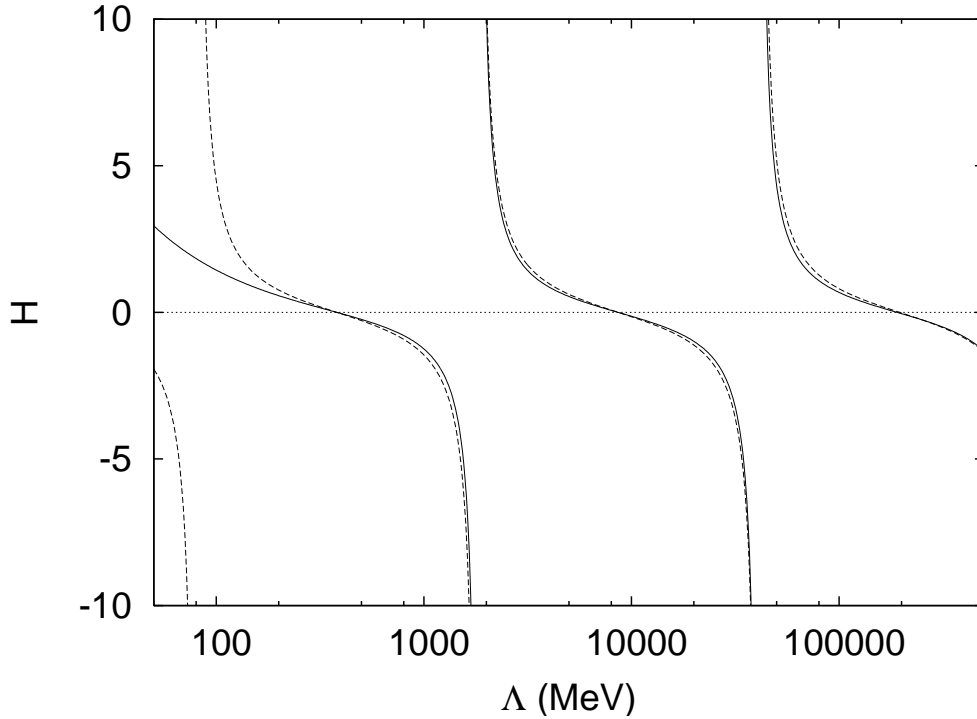


FIG. 5: Values of the three-body force H as a function of the cutoff Λ in MeV. For comparison, the dashed curve shows the asymptotic, scale-free form of $H(\Lambda)$.

the presence of the Efimov effect in this three-body system, a tower of deeply bound states with energies in a constant ratio [15]. In three-nucleon systems only the shallowest of these states lies within the domain of the EFT and so corresponds to a physical state.

The asymptotic form of $H(\Lambda)$ in this limit is [8]

$$H(\Lambda) = -\frac{\sin[s_0 \ln(\Lambda/\Lambda_*) - \arctan(1/s_0)]}{\sin[s_0 \ln(\Lambda/\Lambda_*) + \arctan(1/s_0)]}. \quad (41)$$

where $s_0 = 1.00624 \dots$ and the scale parameter Λ_* is defined by

$$\Lambda_0 = \Lambda_* \exp[(1/s_0) \arctan(1/s_0)]. \quad (42)$$

This form is shown by the dashed line in Fig. 5. The numerical results deviate from it only for small values of Λ where the finite scattering lengths can influence the renormalisation of the three-body force.

B. ^3He channel

For the ^3He channel, we need to the pp Coulomb scattering length as a two-body input parameter,

$$a_C = -7.8063 \pm 0.0026 \text{ fm} \quad [29]. \quad (43)$$

The experimental binding energy of ^3He is

$$B_3(^3\text{He}) = 7.71804 \text{ MeV}, \quad (44)$$

corresponding to a scale $\alpha = 85.127 \text{ MeV}$

As already noted, the $K^{(d,V)}$ term contains a logarithmic singularity that needs to be dealt with carefully. We handle it with the method outlined in Appendix B in Ref. [20]. In the case of a bound state, the other factors in the integral are regular and so the logarithmic singularity has a finite integral. We can take the interval around the singular point and, treating the other factors as constant, explicitly integrate the logarithm over it. The result can be expressed in a similar form to a Gaussian quadrature,

$$\int_a^b dq \ln(p_j - q)^2 y(q) = \sum_{i \neq j}^N w_i \ln(p_j - q_i)^2 y(q_i) + w'_j y(p_j), \quad (45)$$

where $y(q)$ is a smooth function and the w_i are the usual weights. The modified weight for the singular point is given by

$$\begin{aligned} w'_j &= \int_{q_{j<}}^{q_{j>}} dq \ln(p_j - q)^2 \\ &= -2w_j + 2(q_{j>} - p_j) \ln(q_{j>} - p_j) + 2(p_j - q_{j<}) \ln(p_j - q_{j<}), \end{aligned} \quad (46)$$

where $q_{j<} = a + \sum_{k=1}^{j-1} w_k$ and $q_{j>} = a + \sum_{k=1}^j w_k$.

To examine the size of Coulomb effects in the three-nucleon system, we first consider an isospin-symmetric three-body force and take $H(\Lambda_0)$ for the same value $\Lambda_0 = 380.689 \text{ MeV}$ as in the triton. We use $N_4 = 32$ Gaussian points for the four integrals needed to evaluate the kernels $K^{(c)}$ and $K^{(d)}$. The integral equations are discretised using up to $N = 32$ points (leading to 96×96 matrices). We fit the results for $N = 16$ and 32 to the form $\alpha(N) \simeq A + B/N$ in order to extrapolate to $N = \infty$.

Using the first choice for the discretisation variable ($p = m \tan(x)$), we get $\alpha = 84.8084 \text{ MeV}$, or a binding energy of $B_3 = 7.66038 \text{ MeV}$. This differs from the triton energy

for the same three-body force by 0.82 MeV. It is within 1% of the observed ${}^3\text{He}$ energy, indicating that the isospin-violating three-body force is indeed a higher-order contribution. This is as expected, given the absence of any modification of the renormalisation, since the isospin-violating term is suppressed by one power of the inverse Bohr radius κ relative to the LO force.

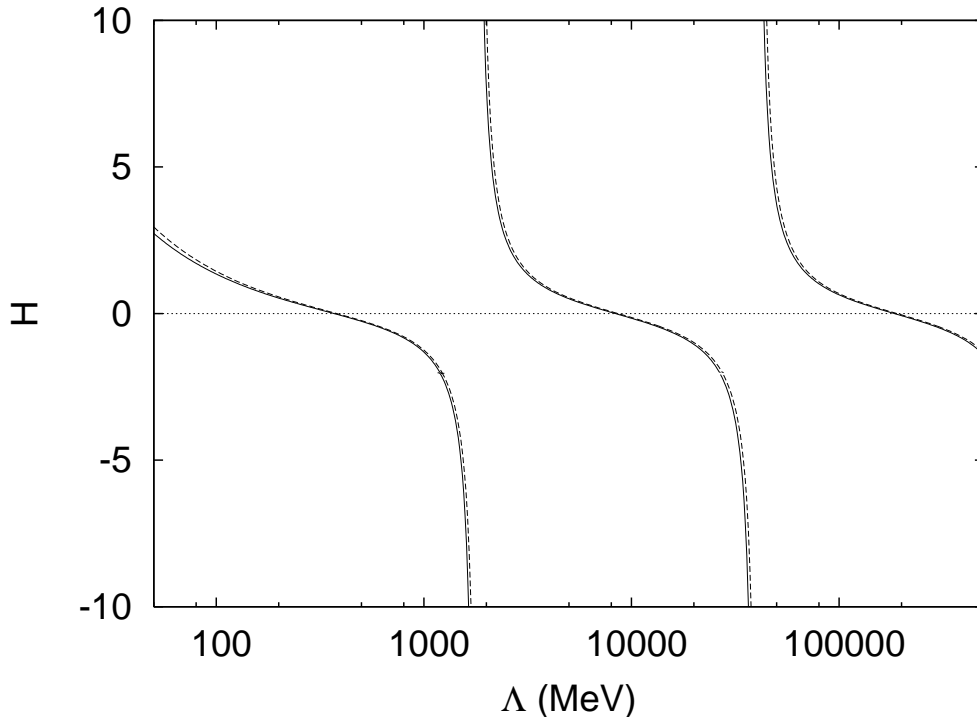


FIG. 6: Evolution with Λ of the three-body forces $H(\Lambda)$ for ${}^3\text{He}$ (solid line) and the triton (dashed).

Our difference between the triton and ${}^3\text{He}$ binding energies is significantly larger than the 0.66 ± 0.03 MeV found by Kirscher *et al.* [19]. However, although working to NLO, those authors took a charge-independent value for the 1S_0 scattering length. Their results are consistent with other estimates of the pure Coulomb contribution [30, 31].

Because we take different values for the nn and np 1S_0 scattering lengths, our calculations do include some higher-order isospin-breaking effects. Given that we have not done a consistent calculation to N²LO (or even NLO), the best we can say is that the ~ 160 keV difference between our result and that of Ref. [19] is comparable in size to the contributions of 70–110 keV that have been estimated using other approaches [30–33]. One caveat that should be made about these comparisons is that, as noted above, there is no model-independent way to separate Coulomb and other isospin-breaking effects in this EFT.

By adjusting the strength of the three-body force, we can fit the experimental binding energy. As in the triton case, we have done this for a range of cutoffs. The results are plotted in Fig. 6. They display the same limit-cycle behaviour as in the triton channel. Moreover the differences between the forces needed in the two channels are very small, reflecting the fact that a symmetric force can give a very good account of ${}^3\text{He}$.

To quantify the size of the isospin breaking in the three-body forces, it is better not to consider the values of $H(\Lambda)$, since these cycle between $\pm\infty$. The scale Λ_0 or, equivalently Λ_* , is a more appropriate measure. Its value of $\Lambda_0 = 382.46$ MeV differs from that for the triton by 0.46%. The contribution of this force to the triton- ${}^3\text{He}$ splitting is about 50 keV. This is much larger than the 5 keV estimate of the three-body contribution in Ref. [33], which may reflect the fact that other isospin-breaking effects are missing from our calculation. Also, the results of Ref. [33] were obtained using an EFT that includes pion fields.

V. SUMMARY

We have studied ${}^3\text{He}$ within the framework of the pionless EFT, treating the Coulomb interaction nonperturbatively. We solve the set of integral equations developed by Kok *et al.* [20], which can be thought of as extending the equation of Skornyakov and ter-Martirosian [21] to include the full off-shell Coulomb T -matrix.

We find that a three-body interaction is required at leading order in ${}^3\text{He}$, as in the triton. This force also exhibits the same limit-cycle behavior as a function of the cutoff Λ as found by Bedaque *et al.* [8] for systems with purely short-range interactions. These results show that the Coulomb interaction is not singular enough to alter the deeply bound “Efimov” states in the three-nucleon system.

We find that an isospin symmetric three-body force, fit to the triton binding energy, can give the ${}^3\text{He}$ binding to better than 1%. The scale parameter of the force that fits ${}^3\text{He}$ differs from the corresponding value for the triton by about 0.5%. This is of the expected size for an order- α electromagnetic effect.

Our results demonstrate that the Coulomb interaction has no nonperturbative effect on the renormalisation of the three-body force in ${}^3\text{He}$. Moreover the overall contributions of the Coulomb interaction to the binding energy of ${}^3\text{He}$ are small, perhaps unsurprisingly given the typical momenta involved, and so could have been calculated perturbatively. This will

not be the case if our approach is extended to describe low-energy pd scattering. However, as noted above, such an extension will require improved numerical techniques to handle the singularity of the Coulomb interaction.

Our approach could also be used to determine the ^3He wave function from the corresponding eigenvector of the set of integral equations. This could then be used in calculations of electromagnetic properties of ^3He , based on the methods in Ref. [34].

Our present results do include certain other isospin-breaking effects beyond LO in this EFT, through the nn and np 1S_0 scattering lengths. A proper treatment of these in the three-nucleon system will require a consistent higher-order calculation. We have provided here the basic forms of the integral equations allowing for isospin-breaking in the NN scattering lengths. The relevant power counting for the terms needed in a full calculation can be determined using the techniques in Refs. [35, 36].

Acknowledgments

This work was supported by STFC grants PP/F000448/1 and ST/F012047/1. We are grateful to L. Kok and his colleagues in Groningen for providing copies of the reports [20].

-
- [1] S. Weinberg, Phys. Lett. **B251**, 288 (1990); Nucl. Phys. **B363**, 3 (1991).
 - [2] S. R. Beane, P. F. Bedaque, W. C. Haxton, D. R. Phillips and M. J. Savage, *At the frontier of particle physics: handbook of QCD*, ed. M. Shifman, vol. 1, p. 133 (World Scientific, Singapore, 2001).
 - [3] P. F. Bedaque and U. van Kolck, Ann. Rev. Nucl. Part. Sci. **52**, 339 (2002).
 - [4] E. Epelbaum, Prog. Part. Nucl. Phys. **57**, 654 (2006).
 - [5] P. F. Bedaque and U. van Kolck, Phys. Lett. **B428**, 221 (1998).
 - [6] U. van Kolck, Nucl. Phys. **A645**, 273 (1999).
 - [7] D. B. Kaplan, M. J. Savage, and M. B. Wise, Phys. Lett. **B424**, 390 (1998); Nucl. Phys. **B534**, 329 (1998).
 - [8] P. F. Bedaque, H.-W. Hammer and U. van Kolck, Nucl. Phys. A **676**, 357 (2000).
 - [9] H. A. Bethe, Phys. Rev. **76**, 38 (1949).

- [10] X. Kong and F. Ravndal, Phys. Lett. **B450**, 320 (1999).
- [11] X. Kong and F. Ravndal, Phys. Rev. C **64**, 044002 (2001).
- [12] T. Barford and M. C. Birse, Phys. Rev. C **67**, 064006 (2003).
- [13] S. Ando, J. W. Shin, C. H. Hyun and S.-W. Hong, Phys. Rev. C **76**, 064001 (2007).
- [14] S. Ando and M. C. Birse, Phys. Rev. C **78**, 024004 (2008).
- [15] V. N. Efimov, Sov. J. Nucl. Phys. **12**, 589 (1971); **29**, 546 (1979).
- [16] E. Braaten and H.-W. Hammer, Phys. Rev. Lett. **91**, 102002 (2003).
- [17] G. Rupak and X. Kong, Nucl. Phys. **A717**, 73 (2003).
- [18] H.-W. Hammer and R. Higa, Eur. Phys. J. **A37**, 193 (2008).
- [19] J. Kirscher, H. W. Griesshammer, D. Shukla and H. M. Hofmann, Eur. Phys. J. A **44**, 239 (2010).
- [20] L. P. Kok, D. J. Struik, and H. van Haeringen, University of Groningen Internal Report 151 (1975); L. P. Kok, D. J. Struik, J. E. Holwerda and H. van Haeringen, University of Groningen Internal Report 170 (1975).
- [21] G. V. Skorniakov and K. A. Ter-Martirosian, Sov. Phys. JETP, 648 (1957).
- [22] S. Ando and C. H. Hyun, Phys. Rev. C **72**, 014008 (2005).
- [23] M. C. Birse, J. A. McGovern and K. G. Richardson, Phys. Lett. **B464**, 169 (1999).
- [24] M. C. Birse, in *Proc. of the 6th International Workshop on Chiral Dynamics*, PoS(CD09)078 (2009).
- [25] J. Gasser and H. Leutwyler, Phys. Rep. **87**, 77 (1982).
- [26] J. C. Y. Chen and A. C. Chen, Adv. Atom. Mol. Phys. **8**, 71 (1972).
- [27] L. Koester and W. Nistler, Z. Phys. A **272**, 189 (1975).
- [28] G. F. de Téramond and B. Gabioud, Phys. Rev. C **36**, 691 (1987).
- [29] J. R. Bergervoet, P. C. van Campen, T. A. Rijken and J. J. de Swart, Phys. Rev. C **38**, 770 (1988).
- [30] S. A. Coon and R. C. Barrett, Phys. Rev. C **36**, 2189 (1987).
- [31] Y. Wu, S. Ishikawa and T. Sasakawa, Phys. Rev. Lett. **65**, 3160 (1990); **66**, 242 (1991).
- [32] R. Machleidt and H. Mütter, Phys. Rev. C **63**, 034005 (2001).
- [33] J. L. Friar, G. L. Payne and U. van Kolck Phys. Rev. C **71**, 024003 (2005).
- [34] H. Sadeghi and S. Bayegan, Nucl. Phys. **A753**, 291 (2005); H. Sadeghi, S. Bayegan and H. W. Griesshammer, Phys. Lett. **B643**, 263 (2006).

- [35] P. F. Bedaque, H. W. Griesshammer, H.-W. Hammer and G. Rupak, Nucl. Phys. **A714**, 589 (2003).
- [36] T. Barford and M. C. Birse, J. Phys. A: Math. Gen. **38**, 697 (2005).